Int. J. Electrochem. Sci., 14 **(2019)** 2621 – 2630, doi: 10.20964/2019.03.70

International Journal of
ELECTROCHEMICAL
SCIENCE
www.electrochemsci.org

Short Communication

Effect of Antimony (III) on Tin Recovery by Cementation on Zinc Powder under Alkaline Conditions

Ping Luo, Bin-bin Sun, Ji-xiu Li, Meng-tian Lu, Li-zhang Wang, and Jia-chao Jiang[*]

School of Environment Science and Spatial Informatics, China University of Mining and Technology, Xuzhou 221116, China
[*]E-mail: jiangjiachao@cumt.edu.cn, ping.luo@live.cn

Received: 5 November 2018 / *Accepted:* 19 December 2018 / *Published:* 7 February 2019

The cementation recovery of tin (Sn) from industrial waste is important in meeting fast-growing demand. However, Sn recovery from alkaline solutions using zinc (Zn) powder is inefficient due to the compact layer of Sn formed on the surface of Zn powder which significantly inhibits the cementation reaction. The presence of a suitable activator could address this resulting in sustainable reactions between Sn^{4+} and Zn powder under alkaline conditions. The aim of this study was to investigate the effects of the addition of an additive (Sb^{3+}) on the recovery of Sn. Cementation experiments were carried out in alkaline solution using dendritic Zn powders in the presence and absence of Sb^{3+}. The mechanism was proposed using electrochemical testing, including cathodic and anodic polarization measurements. The results demonstrated that the presence of Sb^{3+} increased the ratio of the cementation electromotive force (EMF) and the reduction current of the Sn deposition in the cathode, producing more dispersed Sn particles and H_2 gas. This method significantly reduced Sn depositing on the surface of Zn powder, which increased the cementation efficiency and reduced the reaction time. Metallic Sn with high purity (98.53%) and recoverable cemented solution (containing 94 mg/L Sn^{4+}) were achieved within 45 min using the optimal Zn/Sn molar ratio (2.60:1.00) in the presence of the optimal Sb^{3+} concentration (100 mg/L).

Keywords: tin cementation; zinc powder; alkaline solution; Sb^{3+} additive

1. INTRODUCTION

Tin (Sn) is used extensively for commercial and industrial purposes due to its malleability, ductility, elongation and resistance to corrosion [1]. The widespread use and diverse application of Sn creates a high production demand, which is expected to grow by 2% per year over the next 5-10 years. Currently Sn is produced in approximately equal quantity from ores and secondary sources (recycled materials), producing approximately 300,000 tons per year [2-5]. There is a shortage of tin-ore

resources resulting in the focus of Sn recovery from secondary sources, such as waste printed circuit boards (WPCBs) [6], tin slag [7] and electroplating sludge [8].

Hydrometallurgical processes are generally energy-efficient and environment-friendly for the leaching of Sn from industrial waste in alkaline or acidic solutions, which is followed by precipitation, electrolysis or cementation (metal displacement). Cementation has been widely used due to its environmental compatibility [9]. It is a spontaneous electrochemical reduction process, during which a metal ion contained in a liquid phase is reduced onto a more electronegative metal [10, 11]. Cementation recovery of Sn in acidic solutions is extensively reported in the literature [12, 13]. The feasibility of Sn powder production using Zn or Al powders as sacrificing metals [12] and the recovery of Sn powder from acidic $SnCl_2$ solution using Zn powder [13] have been reported. However, other metal ions are also extracted into the solution using acid leaching methods causing impurities. To the best of the authors' knowledge, there are very few reported studies on Sn recovery from alkaline solutions using cementation.

Previously reported work demonstrates a decrease in the concentration of Sn^{4+} to < 100 mg/L using cementation with Zn powder resulting in insignificant contamination of the Zn electrodeposition process [14]. However, the cementation reaction is inefficient due to the compact layer of Sn crystallized on the surface of Zn powder which significantly retards or stops the cementation reaction. The cemented Sn coats unreacted Zn powder which further agglomerates together in a block structure. Therefore, a potential disadvantage of Sn recovery in alkaline solutions by Zn powder is that the cemented metal (Sn) is not pure and large quantities of sacrificing metal (Zn powder) is required. A similar phenomenon is reported in acidic solutions where a compact layer of Sn covered Al in $SnSO_4$ solutions, stopping the cementation reaction [12]. However, after the addition of Cl^-, the cemented Sn was dispersed as powder and the cementation reaction proceeded [12]. A possible explanation for this is that accelerated H_2 evolution passivates the growing crystals and promotes the formation of dendritic Sn particles. Other activators, such as $CuSO_4$, $C_8H_4K_2O_{12}Sb_2$ [15] and Sb_2O_3 [16], are reported to promote cementation in acidic solutions. It is hypothesized that the presence of suitable activators could also promote Sn cementation in alkaline solution.

The aim of this study was to demonstrate the use of an activator in Sn recovery in alkaline solution. The Sn cementation process, purity and size dispersity of the Sn product was investigated in the absence and presence of Sb^{3+} and the possible mechanisms of the cementation promotion were discussed. Zn powder was chosen as the sacrificing metal since it can be recovered directly using electro-wining and reused in conditions where the concentration of Sn^{4+} concentration is < 100 mg/L [17, 18]. The results from preliminary studies using different activators resulted in $C_8H_4K_2O_{12}Sb_2$ being selected to investigate the mechanism of cementation using Zn powder in alkaline solution.

2. EXPERIMENTAL

2.1 Materials

Chemicals and reagents were of analytical grade. Deionized water was used for the preparation of aqueous solutions. Sodium stannate (Na_2SnO_3), zinc oxide (ZnO) and sodium hydroxide (NaOH)

were purchased from Sinopharm (Shanghai, China). Antimony potassium tartrate ($C_8H_4K_2O_{12}Sb_2$) was provided by Zhiyuan (Tianjin, China).

Zinc powder in dendritic structures was synthesized, according to the method by Jiang, with minor modifications, alkaline electro-winning the electrolyte (35 g/L Zn^{2+} and 200 g/L NaOH) at the current density of 1000 A/m^2 for 1 hour [19]. The Zn powder was then removed from the cathode plate, rinsed with deionized water until neutral and dried in the vacuum oven. After grinding with a mortar and sieving through 200 mesh sieves (< 75 μm), the size distribution of the Zn powder was determined using a laser particle size analyzer (S3500, Microtrac, USA). The specific surface area was determined using the surface area and porosimeter analyzer (ASAP2460, Micromeritics, USA). Results of the analysis are shown in Table 1.

Table 1. Size distribution and surface area of Zn powder as determined by laser particle size analyzer and surface area and porosimeter analyzer, respectively

Parameters	Diameter (μm)				Specific surface area (m^2/g)
	D (3, 2)	D (4, 3)	D50	D90	
Values	34.10	56.85	46.11	107.0n	0.5299

Notes: D (3, 2) is the average diameter over area. D (4, 3) is the average diameter over volume. D50 is median diameter, the sieve diameter for 50% of Zn powder passing. D90 is sieve diameter for 90% of Zn powder.

2.2 Cementation experiment

The cementation experiment was carried out in a temperature controlled Plexiglas's reactor fitted with a reflux condenser to avoid the loss of liquid in the form of vapor. Tin reduction (20 g/L Sn^{4+}) in 200 mL alkaline solution (120 g/L NaOH) was performed by the addition of synthesized Zn powder (6.61 g) in the presence or absence of Sb^{3+} for 1 hour under optimum conditions, e.g. 90 ºC, and 500 rpm. Sampling (5 mL) for Sn^{4+}, Zn^{2+} and Sb^{3+} concentration were performed at 15 minute intervals. The concentration of Sn^{4+}, Zn^{2+} and Sb^{3+} were measured using inductively coupled plasma spectrometry (ICP, Perkin Elmer, OPTIMA80000, USA) after acidification with 5% HNO_3 (v/v). At the end of experiment, Sn products were washed out using deionized water until neutral, vacuum oven dried and subdivided into three samples. The first sample was used for digital imaging for size and morphological analysis. The other two samples were sieved using a 100 mesh (< 150 μm). The second sample was prepared for X-ray diffraction (XRD, D8 Advance, Bruker, Germany) to determine the surface composition. The third sample was acidified using 6 mol/L HCl and used to determine impurities by ICP.

2.3 Study of optimum cementation conditions

The optimal additive Sb^{3+} was investigated using a Zn/Sn molar ratio of 3.00:1.00 and different concentrations of Sb^{3+}, such as 0, 50, 100 and 200 mg/L, in the cementation reaction. Once the optimum concentration was determined using the reaction rate constants (k) and Zn powder consumption, different Zn/Sn molar ratios (2.50, 2.55, 2.60, and 3.00) were then used with the optimal concentration of Zn powder.

2.4 Determining the cementation mechanism

Cementation reduction of Sn^{4+} using Zn powder in alkaline solution in the absence and presence of Sb^{3+} was initially determined using theoretical analysis of a Zn-Sn galvanic cell. The standard electromotive force (E_{mf}^{θ}) of the Zn-Sn and Zn-Sb galvanic cell was calculated using electron transfer reaction equations. Further electrochemical investigation of the cementation process in the absence and presence of Sb^{3+} was performed using cathodic and anodic polarization measurements. These experiments were carried out using an electrochemical station (CHI600E, CH Instruments Ins., USA) with a scan rate of 5 mV/s at room temperature (~ 20 ºC). Cathodic polarization measurements were performed in a three-electrode cell using a sweeping voltage from -0.8 V to -1.8 V and a working electrode of Sn foil (with an exposed area of 4 cm^2), a Hg/HgO reference electrode and a Pt plate (4 × 4 cm) being the counter electrode. Anodic polarization tests were conducted in the same three-electrode cell, with the voltage ranging from -1.5 V to -1.3 V, with a working electrode of Zn foil (an exposed area of 4 cm^2), Hg/HgO reference electrode and Sn foil (4 × 4 cm) counter electrode.

3. RESULTS AND DISCUSSION

3.1 Effect of Sb^{3+} *on the process of Sn cementation*

3.1.1. Characteristics of Sn cementation process

The characteristics of Sn cementation process are presented in Table 2 as reaction rate constants (k), time consumed to reduce $C_{Sn^{4+}}$ from 20,000 mg/L to 100 mg/L, Zn loss for hydrogen evolution. The rate constant (k) significantly increased along with the increment of Sb^{3+} concentration from 50 mg/L to 200 mg/L. Sn^{4+} concentration in alkaline solution was reduced to < 100 mg/L within 45 min in the presence of any concentrated Sb^{3+} while the Sn^{4+} concentration was constantly > 1000 mg/L over the whole experimental period in the absence of Sb^{3+} (approximately 4 hours). Bubbles were observed with naked eyes during the cementation process with zinc powders in the presence and absence of Sb^{3+}. More bubbles were observed along with the increment of Sb^{3+} (Table 2). With addition of 50, 100, 200 mg/L of Sb^{3+}, calculated Zn loss (%) that contributed to hydrogen evolution were 0.86, 2.82, 5.72 times higher, respectively, than in the absence of Sb^{3+} (Table 2).

The results showed that the addition of Sb^{3+} has significantly enhanced the cementation efficiency as well as reduced reaction time. In regards to the time consumption to reduce $C_{Sn^{4+}}$ from 20,000 mg/L to 100 mg/L in the absence of Sb^{3+}, it was much longer than our previous published work (8 hours) [14]. This was because we used dendritic zinc powders here while spherical particles were used in previous work. Hydrogen evolution can take place between Zn powder and alkaline solution without Sb^{3+} due to the reaction between zinc powders and hydroxyl ion in alkaline solution (Equation 1) [20, 21]. The presence of Sb^{3+} has significantly accelerated zinc consumption and promoted hydrogen evolution (more bubbles). More dispersed Sn particles were therefore observed with the increment of Sb^{3+} addition.

We also found a large quantity of Sb^{3+} eliminated out from the alkaline solution during reaction. It was suspected that the Sb^{3+} was also cemented by Zn powder which might potentially affect the purity of the tin product [22]. Medium tested concentration, 100 mg/L Sb^{3+}, was hence selected for the following impurities study.

$$\mathrm{Zn(s)} + 2OH^-(aq) \rightarrow \mathrm{Zn}O_2^{2-}(aq) + H_2\mathrm{(g)} \quad (1)$$

Table 2. Characteristics of Sn cementation process using Zn powder in alkaline solution in the presence and absence of Sb^{3+}.

Sb^{3+} concentration (mg/L)	k[1] (s^{-1}, 10^{-3})	Time[2] (min)	Zn (H_2)[3] (%)	H_2 evolution[4] (mg)	Sn dispersion
0	0.498	-	2.79	5.63	in block form
50	1.012	45	5.19	10.50	weakly dispersed
100	1.156	45	10.66	21.55	dispersed
200	1.314	45	18.75	37.92	well dispersed

Note: [1] cementation rate constant k

[2] time consumed to reduce $C_{Sn^{4+}}$ to < 100 mg/L

[3] calculated Zn loss (%) for hydrogen evolution

[4] calculated mass of H_2 evolution

3.1.2 Impurities estimation

Table 3 shows data for impurities analysis of tin along variable sacrificing mental (Zn powder) dosage in presence of optimum Sb^{3+} (100 mg/L). More addition of sacrificing metal (Zn) from one side can promote the cementation reaction and left less Sn^{4+} in alkaline solution. Once the Zn/Sn molar ratio increased to 2.60:1.00, the remaining Sn^{4+} concentration in solution decreased to < 100 mg/L where Zn can be effectively recovered at the end of commendation process [14]. From the other side, the addition of more Zn powder can also reduce the Sn purity. Only 81.93% of tin purity was observed in the cemented metal at Zn/Sn molar ratio of 3.00:1.00. Therefore, Zn/Sn molar ratio of 2.60:1.00 was recommended since it can produce high purity of the metallic tin (98.53%) and recoverable cemented solution (containing 94 mg/L Sn^{4+} ions).

Table 3. Effects of Zn dosage on the cementation reduction of Sn.

Zn/Sn (molar ratio)	2.50:1.00	2.55:1.00	2.60:1.00	3.00:1.00
Remaining Sn^{4+} (mg/L)	143	118	94	86
Sn content of the cemented Sn (wt.%)	/	/	98.53%	81.93%

Figure 1 shows typical XRD patterns of the cemented tin products on zinc with optimum Zn/Sn molar ratio (2.60:1.00) in the absence and presence of optimum Sb^{3+} (100 mg/L). Apart from the diffraction peaks of tin, diffraction peaks assigning to the hexagonal crystalline zinc (JCPDS 04-0831) [13] were found in the absence of Sb^{3+} (Figure 1a). With the addition of 100 mg/L Sb^{3+}, only diffraction peaks indexing to the tetragonal crystalline tin (JCPDS 86-2264) [13, 23] were found. No characteristic peaks of Zn were observed (Figure 1b). It indicates the high purity of tin product obtained using optimum Zn/Sn molar ratio (2.60:1.00) in the presence of optimum Sb^{3+} (100 mg/L).

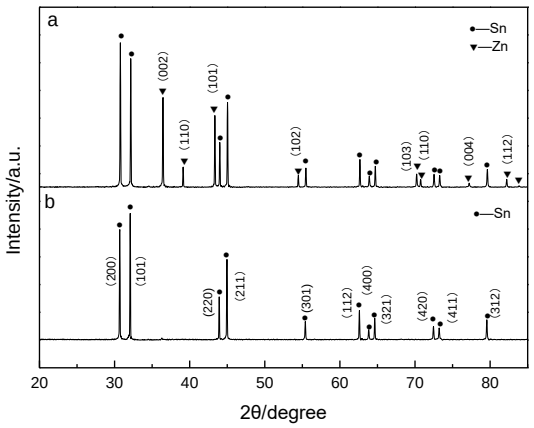

Figure 1. X-ray diffraction (XRD) patterns of Sn products in the absence (a) and presence (b) of optimum Sb^{3+} (100 mg/L), where 20 g/L of Sn^{4+} was reduced by 5.73 g Zn powder (optimum molar ratio of Zn:Sn, 2.60:1.00) in 200 mL alkaline solutions (120 g/L NaOH) for 1 hour under the optimum conditions, e.g. 90 ºC), 200mL solution volume and 500 rpm.

3.1.3 Morphology of cemented tin

Figure 2 shows the morphological change of cemented Sn using optimum Zn/Sn molar ratio (2.60:1.00) in the absence and presence of optimal concentration of Sb^{3+} (100 mg/L). In the absence of Sb^{3+}, a large non-uniform spherical shape of Sn deposit occurred (Figure 2a). Significantly fine granules were found in the presence of 100 mg/L Sb^{3+} (Figure 2b). In agreement with additive optimum study (Table 2), the results suggest that the addition of 100 mg/L Sb^{3+} can significantly reduce the size of Sn particles. A possible reason is the formation of a compact layer of Sn on the surface of Zn powder in the absence of Sb^{3+}. Unreacted Zn powder was rapidly coated by Sn, forming a spherical structure as a result of the ductility of Sn at high temperatures. The contact between the solution and Zn powder was inhibited due to the increased liquid-solid diffusional resistance. The cementation reaction rate therefore decreased or stopped (Table 2).

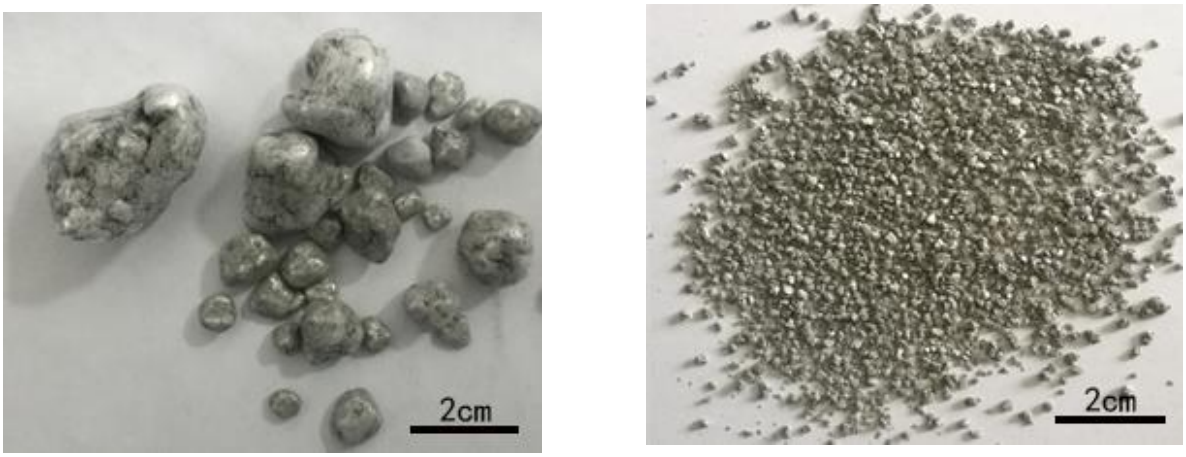

(a) (b)

Figure 2. The morphology of cemented Sn in the absence (a) and presence (b) of optimal Sb^{3+} (100 mg/L), where 20 g/L of Sn^{4+} was reduced by 5.73 g Zn powder (optimal molar ratio of Zn:Sn, 2.60:1.00) in 200 mL alkaline solution (120 g/L NaOH) for 1 hour under the optimum conditions (90 ºC), and 500 rpm).

The addition of additive can significantly enhance the cementation efficiency, increasing the rate of the Sn cementation process, and improving Sn purity and size dispersion. The optimal cementation conditions were 100 mg/L Sb^{3+}, Zn:Sn molar ratio of 2.60:1.00, 90 ºC) and 500 rpm.

3.2 Mechanism of cementation

3.2.1 Theoretical analysis of the cementation reduction of Sn

To further identify the electrochemical mechanisms of the cementation reduction of Sn using Zn powder in alkaline solutions, a theoretical analysis of a Zn-Sn galvanic cell in the absence of Sb^{3+} was initially performed. The overall cell reaction was:

$$[Sn(\mathrm{OH})_6]^{2-}(\mathrm{aq}) + 2Zn(\mathrm{s}) + 2OH^-(\mathrm{aq}) \rightarrow 2\mathrm{Zn}(OH)_4^{2-}(\mathrm{aq}) + Sn(\mathrm{s}) \quad (2)$$

The electron transfer reaction equations and the corresponding standard electrode potentials are [24]:

$$[Sn(\mathrm{OH})_6]^{2-}(aq) + 2e^- \rightarrow HSnO_2{}^-(aq) + H_2\mathrm{O} + 3OH^-(aq), E^\theta([Sn(\mathrm{OH})_6]^{2-}|HSnO_2{}^-) = -0.93\ \mathrm{V} \quad (3)$$

$$HSnO_2{}^-(aq) + H_2\mathrm{O} + 2e^- \rightarrow \mathrm{Sn(s)} + 3OH^-(aq), E^\theta(HSnO_2{}^-|\mathrm{Sn}) = -0.909\ \mathrm{V} \quad (4)$$

$$[Sn(\mathrm{OH})_6]^{2-}(aq) + 4e^- \rightarrow \mathrm{Sn(s)} + 6OH^-(aq), E^\theta([Sn(\mathrm{OH})_6]^{2-}|\mathrm{Sn}) \quad (5)$$

$$Zn(\mathrm{OH})_4^{2-}(aq) + 2e^- \rightarrow Zn(\mathrm{s}) + 4OH^-(aq), E^\theta(\mathrm{Zn}(OH)_4^{2-} \mid \mathrm{Zn}) = -1.199\ \mathrm{V} \quad (6)$$

Equations (3) and (4) are the half equations of Equation (5) and the standard electrode potential of Equation (5) can be calculated using the formulae (A) and (B). The $E^\theta([Sn(\mathrm{OH})_6]^{2-}|\mathrm{Sn})$ value is -0.920V.

$$\Delta_r G_m^\theta = -nE^\theta F \quad (A)$$

$$\Delta_r G_m^\theta(\text{Equation (5)}) = \Delta_r G_m^\theta(\text{Equation 3}) + \Delta_r G_m^\theta(\text{Equation 4}) \quad (B)$$

Zn-Sn contact galvanic pair ($Zn|Zn(OH)_4^{2-}||[Sn(OH)_6]^{2-}|Sn$) was the net redox reaction of Sn reduction (Equation 5) and Zn oxidization (Equation 6). The value of the standard electromotive force ($E_{mf}^{\theta}(Zn/Sn)$) of the Zn-Sn galvanic cell was calculated to be +0.279 V (Equation 7) and standard Gibbs free energy was negative ($\Delta_r G_m^{\theta} = -nE_{mf}^{\theta}F < 0$). Hence, a spontaneous heterogeneous reaction occurred in the Zn-Sn galvanic cell, indicating that Zn powder can cement Sn in alkaline solution in the absence of Sb^{3+} [9].

$$E_{mf}^{\theta}(Zn/Sn) = E^{\theta}([Sn(OH)_6]^{2-}|Sn) - E^{\theta}(Zn(OH)_4^{2-}|Zn) = -0.920V-(-1.199V) = +0.279\ V \quad (7)$$

In the presence of Sb^{3+}, the standard electromotive force ($E_{mf}^{\theta}(Zn/Sb)$) of the Zn-Sb galvanic cell was calculated to be +0.539 V (Equation 8), significantly higher than the standard electromotive force ($E_{mf}^{\theta}(Zn/Sn)$) in the absence of Sb^{3+} (+0.279 V). Therefore, Sb^{3+} was cemented by Zn powder preferentially in the early stages of the cementation process. The deposited Sb formed a substrate on the Zn powder surface. Tin was then deposited onto the Sb substrate with an increased Sn content nucleate [22]. Once a Sn-rich nucleus was formed, it developed into a crystal maintaining its high Sn content. More and smaller Sn powder was subsequently produced.

$$E_{mf}^{\theta}(Zn/Sb) = E^{\theta}(SbO_2^{-}|Sb) - E^{\theta}(Zn(OH)_4^{2-}|Zn) = -0.66V-(-1.199V) = +0.539\ V \quad (8)$$

3.2.2 Electrochemical investigation of the cementation process

Figure 3 shows the potentiodynamic polarization curves (a/b) of Sn reduction and Zn corrosion in alkaline solution in the absence and presence of 100 mg/L Sb^{3+}. The addition of 100 mg/L Sb^{3+} significantly inhibited the reduction current density of Sn^{4+}, however the oxidation-reduction potential of Zn and Sn did not change significantly. In agreement with the literature, this increased the ratio of the cementation electromotive force (EMF) and the reduction current of Sn deposition, consequently increasing the ratio of particle nucleation rates and further growth [12]. Over time, smaller Sn powder was produced (Table 2 and Figure 2b).

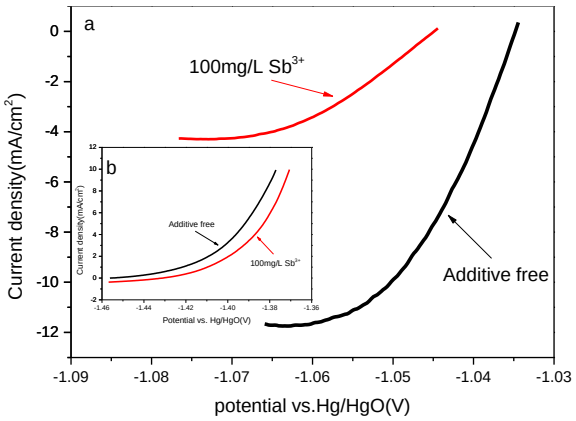

Figure 3. Cathodic potentiodynamic polarization curves of Sn reduction (a) and anodic potentiodynamic polarization curves of Zn corrosion (b) in alkaline solution in the absence and presence of 100 mg/L Sb^{3+} at room temperature (~ 20 ºC)), where 20 g/L of Sn^{4+} in alkaline solution (120 g/L NaOH). The scan rate was 5 mV/s.

Figure 4 shows the variation in H_2 evolution potential in the absence and presence of 100 mg/L Sb^{3+}. The overpotential of H_2 evolution at the beginning of the rapid current increase shifted from -1.60 V (point B) to -1.50 V (point A) after the addition of 100 mg/L Sb^{3+}. The more positive overpotential caused the intensive H_2 evolution in the Sn deposit, resulting in a decrease in the adhesion of Sn deposited onto the Zn surface [25]. This reduced Sn depositing on the surface of Zn powder, prevented block structure agglomerating, and increased Sn dispersion (Table 2 and Figure 2b).

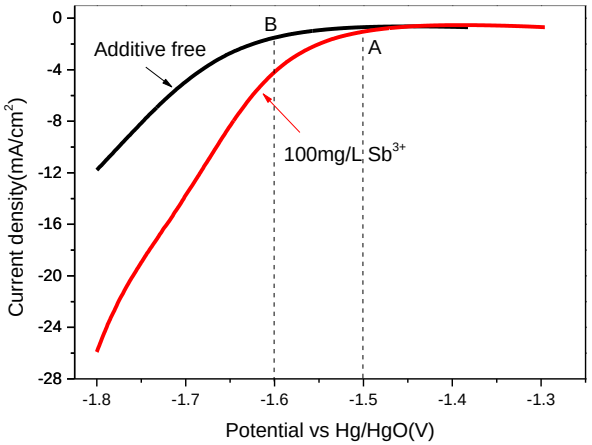

Figure 4. Cathodic curves of H_2 evolution in alkaline solution in the absence and presence of 100 mg/L Sb^{3+} at room temperature (~ 20 ºC)), where 20 g/L of Sn^{4+} in alkaline solution (120 g/L NaOH). The scan rate was 5 mV/s. Point A (-1.5 V) and B (-1.6 V) is the overpotential of H_2 evolution at the beginning of the rapid current in the presence and absence of Sb^{3+}.

Overall, the presence of Sb^{3+} significantly increased the rate of the cementation reaction and produced more dispersed Sn particles. This could be due to the addition of Sb^{3+} into an alkaline solution increasing the ratio of the cementation EMF and the reduction current of the Sn deposition, consequently increasing the ratio of Sn particle nucleation rates and growth. Another explanation could be that the H_2 evolution potential was more positive, resulting in increased H_2 evolution (bubbles) and decreased Sn deposit adhesion to the Zn surface. Instead of forming a compact layer, coating unreacted Zn powder and stopping the reaction, the addition of Sb^{3+} produced more dispersed particles and greatly reduced the chance of Sn depositing onto the surface of Zn powder. Eventually, sustainable reactions between Sn^{4+} and Zn powder in alkaline solution occurred.

4. CONCLUSIONS

This study investigated the effect of Sb^{3+} on tin recovery by cementation on zinc powder under alkaline conditions. This approach significantly increased the efficiency of cementation and reduced the reaction time. High purity of metallic Sn (98.53%) and recoverable cemented solution (94 mg/L Sn^{4+}) were achieved within 45 min using optimal Zn/Sn molar ratio (2.60:1.00) in the presence of

optimal Sb^{3+} concentrations (100 mg/L). This study could provide a cost-effective method for recovering high purity Sn from industrial waste containing Sn commercially.

ACKNOWLEDGMENTS
This work was financially supported by Xuzhou Science and Technology Project (KC16SG260) and the Fundamental Research Funds for the Central Universities (2017XKQY95).

References

1. F.A. López, I. García-Díaz, O.R. Largo, F.G. Polonio and T. Llorens, *Miner.*, 8 (2018) 20.
2. L. Sun, Y.H. Hu and W. Sun, *Trans. Nonferrous Met. Soc. China*, 26 (2016) 3253.
3. Q.C. Feng, W.J. Zhao, S.M. Wen and Q.B. Cao, *Sep. Purif. Technol.*, 178 (2017) 193.
4. T. Leistner, M. Embrechts, T. Leißner, S.C. Chelgani, I. Osbahr, R. Möckel, U.A. Peuker and M. Rudolph, *Miner. Eng.*, 96 (2016) 94.
5. S.I. Angadi, T. Sreenivas, H.S. Jeon, S.H. Baek and B.K. Mishra, *Miner. Eng.*, 70 (2015) 178.
6. T.Z. Yang, P.C. Zhu, W.F. Liu, L. Chen and D.C Zhang, *Waste. Manage.*, 68 (2017) 449.
7. A. Jumari, A. Purwanto, A. Nur, A.W. Budiman,M. Lerian and F.A. Paramita, Tin recovery from tin slag using electrolysis method, *The 3rd International Conference on Industrial, Mechanical, Electrical, and Chemical Engineering*, Surakarta, Indonesia, 2018, 5-9.
8. T. Stefanowicz, T. Golik, S. Napieralska-Zagozda and M. Osińska, *Resour. Conserv. Recycl.*, 6 (1991) 61.
9. R. Jhajharia, D. Jain, A. Sengar, A. Goyal and P.R. Soni, *Powder Technol.*, 301 (2016) 10.
10. C.Y. Wang, M.Y. Lu, H.C. Chen and L.J. Chen, *J. Phys. Chem.C*, 111 (2007) 6215.
11. H.H. Li, C.L. Liang, M. Liu, K. Zhong, Y.X .Tong, P. Liu and G.A. Hope, *Nanoscale Res. Lett.*, 4 (2009) 47.
12. V.V. Artamonov, D.R. Moroz, A.O. Bykov and V.P. Artamonov, *Russ J. Non-Ferr. Met+.*, 54 (2013) 128.
13. L. Cao, J. Liu, W. Huang and Z.L. Li, *Appl. Surf. Sci.*, 265 (2013) 597.
14. J.C. Jiang, W. Chen, X. Hu and Y.C. Zhao, Removal of Tin from Alkaline Zinc Solution by Zinc Powder Cementation. *4th International Conference on Bioinformatics and Biomedical Engineering*, Chengdu, China, 2010, 1-4.
15. B.S. Boyanov, V.V. Konareva and N.K. Kolev, *Hydrometallurgy*, 73 (2004) 163.
16. R. Xu, K, Ma, Z, Guo, *Hydrometallurgy*, 82 (2006) 150.
17. Y.C. Zhao and R. Stanforth, *Hydrometallurgy*, 56 (2000) 237.
18. Q. Liu, Y.C Zhao and G.D Zhao, *Hydrometallurgy*, 110 (2011) 79.
19. J.C. Jiang, J. Tong, P. Luo, J.L. Ma, H. Lu, L.Z. Wang and Y.C. Zhao, *Int. J. Electrochem. Sci.*, 13 (2018) 324.
20. T.J. Wu, M.L. Zhang, K.H. Lee, S.I. Kim and Y.H. Choa, *Electrochim. Acta*, 150 (2014) 298.
21. M. Mouanga, P. Bercot, J.Y. Rauch, *Corros. Sci*., 52 (2010) 3984.
22. V.V.D.Pas and D.B. Dreisinger, *Hydrometallurgy*, 43 (1996) 187.
23. N. Arora and B.R. Jagirdar, *Phys. Chem. Chem. Phys.*, 16 (2014) 11381.
24. W.M. Haynes, *CRC Handbook of Chemistry and Physics*, 95th Edition, Crc Press, (2015) Boca Raton, America.
25. M. Karavasteva, *Hydrometallurgy*, 150 (2014) 47.